

# Attenuating surface gravity waves with mechanical metamaterials

F. De Vita,<sup>1, a)</sup> F. De Lillo,<sup>2</sup> F. Bosia,<sup>3</sup> and M. Onorato<sup>2</sup>

<sup>1)</sup>*Dipartimento di Meccanica, Matematica e Management, Politecnico di Bari, Via Re David 200 – 70125 Bari, Italy*

<sup>2)</sup>*Dipartimento di Fisica, Università degli Studi di Torino, Via Pietro Giuria 1, 10125 Torino, Italy*

<sup>3)</sup>*DISAT, Politecnico di Torino, Corso Duca degli Abruzzi 24, 10129 Torino, Italy*

(Dated: 7 January 2022)

Metamaterials and photonic/phononic crystals have been successfully developed in recent years to achieve advanced wave manipulation and control, both in electromagnetism and mechanics. However, the underlying concepts are yet to be fully applied to the field of fluid dynamics and water waves. Here, we present an example of the interaction of surface gravity waves with a mechanical metamaterial, i.e. periodic underwater oscillating resonators. In particular, we study a device composed by an array of periodic submerged harmonic oscillators whose objective is to absorb wave energy and dissipate it inside the fluid in the form of heat. The study is performed using a state of the art direct numerical simulation of the Navier-Stokes equation in its two-dimensional form with free boundary and moving bodies. We use a Volume of Fluid interface technique for tracking the surface and an Immersed Body method for the fluid-structure interaction. We first study the interaction of a monochromatic wave with a single oscillator and then add up to four resonators coupled only fluid-mechanically. We study the efficiency of the device in terms of the total energy dissipation and find that by adding resonators, the dissipation increases in a non trivial way. As expected, a large energy attenuation is achieved when the wave and resonators are characterised by similar frequencies. As the number of resonators is increased, the range of attenuated frequencies also increases. The concept and results presented herein are of relevance for applications coastal protection.

## I. INTRODUCTION

In recent years, the field of mechanical metamaterials and phononic crystals has seen a rapid development and captured increasing interest<sup>1</sup>. They are engineered materials that have been developed to alter the standard properties of wave propagation such as dispersion, refraction or diffraction. Metamaterials are usually arranged in periodic patterns, at scales that are comparable or smaller than the wavelengths of the phenomena they influence. The simplest effect is that when waves propagate in a periodic structure the dispersion relation displays banded structures with frequency regions that are forbidden, called band gaps. This effect, for example, can be obtained in phononic biatomic materials<sup>2</sup>. The concept of metamaterials was first developed in the field of optics<sup>3</sup> and later extended to phononic crystals and elastic waves<sup>2</sup>. Some work on the interaction of gravity waves with a macroscopic periodic structure (a sinusoidal floor) was already considered (see<sup>4,5</sup>). Results indicated the existence of a mechanism of resonant Bragg reflection occurring when the wavelength of the bottom undulation is one half the wavelength of the surface wave. Further studies on the interactions of waves with periodic structures can be found in<sup>6–8</sup>. Other examples of wave manipulation properties, for example cloaking, can be obtained by employing an engineered elastic buoyant carpet placed on water<sup>9</sup> or by a radial arrangement of vertical cylinders<sup>10</sup>.

The interaction of ocean waves with structures is a long standing problem in fluid mechanics<sup>11</sup>. A theoretical approach based on the direct use of the equations of motion, even in their simplified version, is not always feasible, especially

when geometries are not simple and bodies are moving because of hydrodynamical forces. In the latter cases, an experimental approach is not easy as the measurement of pressures and of the velocity field around the moving bodies may not be straightforward. Numerical methods, despite their complexity, often offer an important alternative for studying wave-structure interaction and designing structures. With respect to standard fluid mechanics, the main complication arises because of the presence of a free surface which substantially increases the difficulty of the numerical treatment. Some studies in the literature assume that the flow is irrotational and inviscid so that the potential flow equations can be solved and forces are limited to pressure<sup>12,13</sup>. However, when the goal is to study the overall effect of wave attenuation and the energy dissipated in the bulk of the fluid, vorticity and viscosity cannot be neglected and the full Navier-Stokes equations need to be computed: recent works<sup>14,15</sup> have provided evidence that viscosity plays an important role, especially close to resonant conditions. To this end, Direct Numerical Simulation (DNS) of a free surface flow interacting with a structure represents a powerful tool that can provide a detailed representation of the flow field and of the fluid-structure interaction.

In this work, we consider the interaction of gravity waves with a periodic structure composed by “internal” resonators, i.e. waves interact with submerged harmonic oscillators which are coupled only fluid-mechanically. To begin with, we work in a two dimensional framework; therefore, strictly speaking, our waves are characterised by infinitely long crests and the oscillators are cylinders whose axes are parallel to the crests. We solve the full Navier-Stokes system of equations coupled with the Volume of Fluid (VoF) method for the interface tracking and the Immersed Boundary Method (IBM) for the fluid-structure interaction. The cylinders undergo the hydrodynamic forces (pressure and viscous stress) of the wave

<sup>a)</sup>Electronic mail: francesco.devita@poliba.it

motion and an elastic force which tends to restore the system back to the equilibrium position. The analysis has been conducted for a variable number of resonators per wavelength and varying their natural frequency. It is worth mentioning that the system we are considering is similar to systems for wave energy conversion, on which there is a rich literature ranging from point-absorbers<sup>15–17</sup> to a full modeling of the solid structure<sup>12,18</sup>. However, the focus here is on the interaction of a wave with a periodic structure rather than the conversion of energy from a single oscillator.

## II. METHODOLOGY

### A. The numerical method

We solve the full Navier-Stokes system of equations

$$\rho(\partial_t \mathbf{u} + \mathbf{u} \cdot \nabla \mathbf{u}) = -\nabla p + \nabla \cdot (\mu \mathbf{D}) + \rho \mathbf{g} + \mathbf{f} \quad (1)$$

$$\nabla \cdot \mathbf{u} = 0 \quad (2)$$

with  $\mathbf{u} = (u, w)$  the velocity field,  $p$  the pressure field,  $\mathbf{D}$  the deformation tensor defined as  $D_{ij} = (\partial_i u_j + \partial_j u_i)/2$ ,  $\mathbf{g}$  the gravity vector and  $\mathbf{f}$  the IBM force which enforces the no-slip boundary condition at the solid boundary. The material properties  $\rho$  and  $\mu$  are related to the volume fraction field  $\mathcal{F}(\mathbf{x}, t)$  as

$$\rho(\mathcal{F}) = \mathcal{F} \rho_1 + (1 - \mathcal{F}) \rho_2 \quad (3)$$

$$\mu(\mathcal{F}) = \mathcal{F} \mu_1 + (1 - \mathcal{F}) \mu_2, \quad (4)$$

where  $\rho_1$ ,  $\rho_2$ ,  $\mu_1$  and  $\mu_2$  are the density and viscosity of the two fluids; the volume fraction field (defined as the volumetric ratio of the two fluids in each computational cell) is advected by the flow with the following equation

$$\partial_t \mathcal{F} + \nabla \cdot (\mathcal{F} \mathbf{u}) = 0. \quad (5)$$

The motion of the resonators is given by Newton's law

$$m_i \frac{d^2 X_i}{dt^2} + \kappa_i (X_i - X_{0,i}) = F_i \quad (6)$$

where  $X_i$  is the position of the centre of mass of the  $i$ -th resonator,  $m_i$  its mass,  $\kappa_i$  is the elastic constant,  $X_{0,i}$  the equilibrium position and  $F_i$  the integral of the hydrodynamic forces acting on it. This force is computed by integrating the pressure ( $p$ ) and the viscous stress tensor ( $\boldsymbol{\tau}$ ) over the surface of the solid body as follows:

$$\mathbf{F} = \int_S (\boldsymbol{\tau} - p \mathbf{I}) \cdot \mathbf{n} dS. \quad (7)$$

By computing the force in this way, all terms typically used in the description of point-absorbers (such as viscous damping and radiation damping) are included, and eq.(7) provides a more general and accurate description of the solid body motion.

Modelled in this way, the resonator has a natural frequency  $\omega_r = \sqrt{k/m}$ . In the real system, resonators would correspond

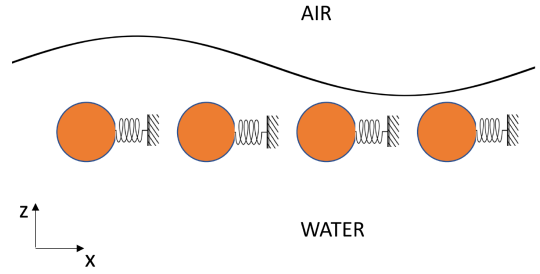


FIG. 1: Sketch of the periodic structure of resonators interacting with a surface gravity wave

to reversed pendula anchored at the bottom; for waves of small amplitude, as in this study, the vertical motion of the resonators can be neglected, hence, we solve equation (6) only for the horizontal motion, with  $F_i$  being the horizontal component of the integral of the hydrodynamic loads acting on the  $i$ -th resonator; the motion in the vertical direction is set to zero.

The Navier-Stokes equations are advanced in time using a 2<sup>nd</sup> order Adams-Bashforth scheme and a fractional step method is employed<sup>19</sup> for the coupling with the pressure; the resulting Poisson equation for the pressure is solved employing a Fast Direct Solver. All derivatives are discretized with a second order central difference scheme apart for the diffusion term in the Navier-Stokes equations, for which a WENO scheme is used<sup>20</sup>. The IBM is implemented using the direct forcing approach<sup>21</sup> with interpolations performed in the direction normal to the interface. For the fluid-structure interaction, a strong coupling is adopted with an iterative solver based on the Hamming method<sup>22</sup>. The solver is limited to non-deformable solid bodies, which allows for more efficient computations. A detailed description of the solver with validations and preliminary results can be found in<sup>23</sup>. A sketch of the periodic structure of four resonators immersed in a fluid and forced by surface gravity waves is displayed in Fig. 1.

### B. Initial conditions

The initial wave profile  $\eta$  and velocity field  $\mathbf{u} = (u, w)$  are taken from linear theory and are, respectively:

$$\eta(x, 0) = a \cos(kx) \quad (8)$$

and

$$u(x, 0) = a \omega e^{kz} \cos(kx) \quad (9)$$

$$w(x, 0) = a \omega e^{kz} \sin(kx), \quad (10)$$

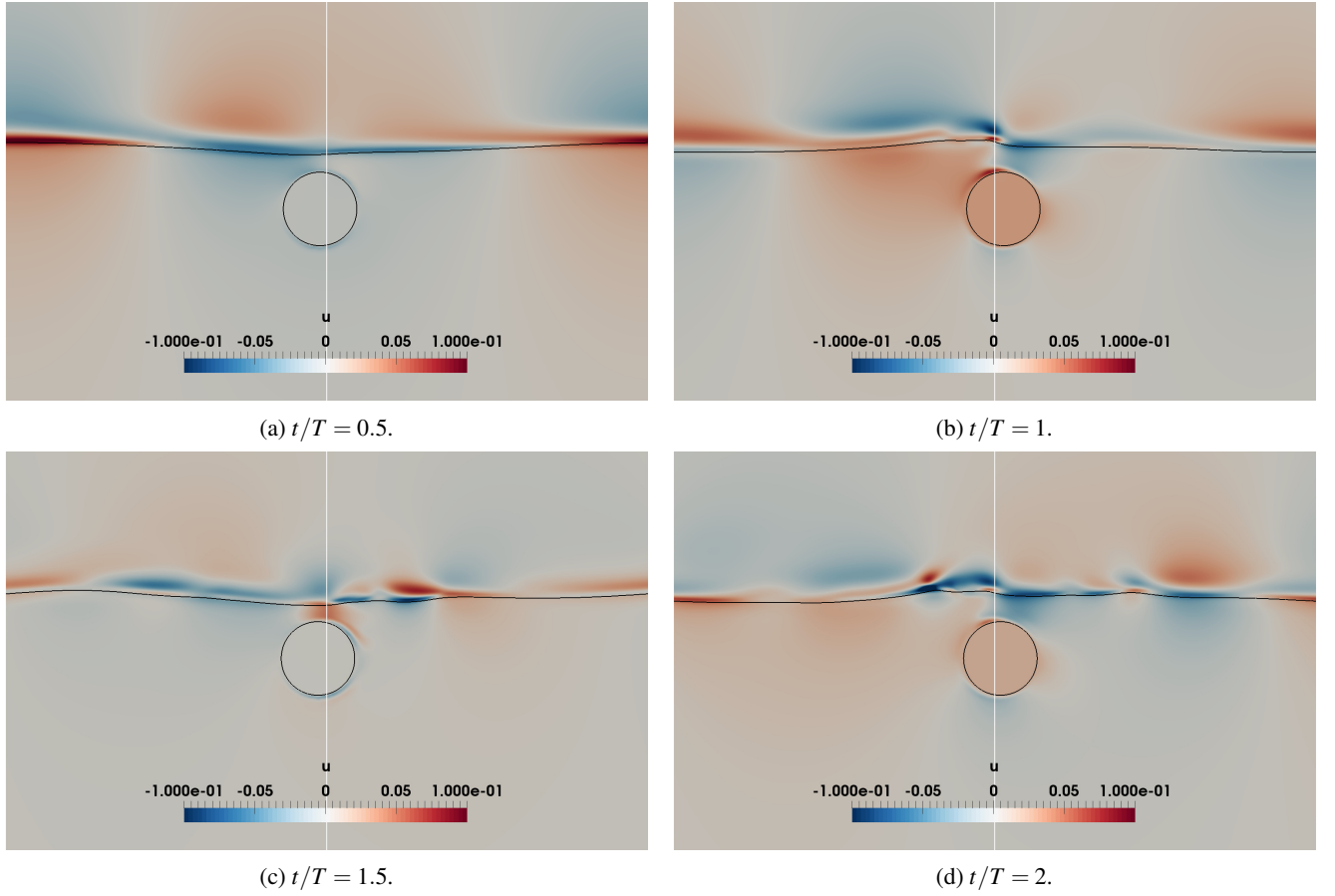


FIG. 2: Snapshot of the horizontal component  $u$  of the velocity field at four instants of time for the case with  $\Omega = 1$ . The vertical white line is located at the center of the domain and it is reported as reference to underline the motion of the resonator. (Multimedia view)

with  $a$  the wave amplitude,  $k = 2\pi/\lambda$  the wavenumber,  $\lambda$  the wavelength and  $z = 0$  the still water level, and  $z$  pointing upward. The wave frequency  $\omega$  is given by the dispersion relation for water waves in deep water  $\omega = \sqrt{gk}$ . The initial velocity field in air is equal to that in water with the horizontal component  $u$  with a negative sign. To avoid high shear stress across the interface at the beginning of the simulation, the initial volume fraction is filtered with a bilinear interpolation which results in a spread of the interface over three cells. Note that this operation is performed only for the initial profile. The computational domain is a square of lateral size  $\lambda$ , the radius of the resonators is  $r = 0.057\lambda$  and the distance from the centre of mass of the resonators and the still water level is  $d = 0.094\lambda$ . The Reynolds number based on the wavelength and phase speed is set to  $Re = \rho g^{1/2} \lambda^{3/2} / \mu = 10^5$ , with  $\rho$  and  $\mu$  the density and viscosity of the high density phase. All simulations are performed with a grid of  $512 \times 512$  computational nodes.

We performed simulations for different numbers of resonators per wavelength and different values of the ratio  $\Omega = \omega_r/\omega$ . The different cases are studied by changing the proper frequency and number of the oscillators, while keeping the amplitude and the length of the initial sinusoidal wave un-

changed. This choice prevents a priori any change in the wave steepness which would in turn affect the nonlinearity of the wave dynamics.

### III. RESULTS

We first consider a single resonator placed at the centre of the domain where a monochromatic wave of wavelength  $\lambda = 1$  (in non dimensional units) propagates. In figure 2 we report the snapshot of the horizontal velocity component  $u$ , the interface location and the oscillator position for the case  $\Omega = 1$  at four instants of time,  $t/T = 0.5, 1, 1.5, 2$ , with  $T$  the wave period. Wave motion forces the resonator to move due to pressure and viscous stresses distribution; the resonator, then, is pulled back to its original position by the elastic force and starts to oscillate around its equilibrium position. This motion induces perturbations on the interface, clearly visible at later stage of the process (figure 2d), leading to vorticity production at the surface which enhances the energy dissipation.

In figure 3 we show the time history of the displacement of the centre of mass of the resonator for  $\Omega = 1$ , i.e. when the frequency of the wave is about the frequency of the res-

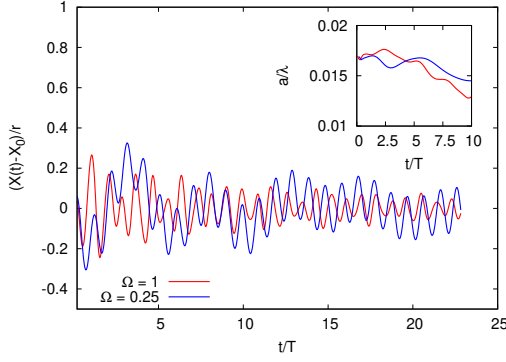


FIG. 3: Time history of the center of mass displacement of one resonator placed in the middle of the domain for two different values of  $\Omega$ ; the inset shows the wave amplitude vs. time for the same cases.

onator, and for  $\Omega = 0.25$ , i.e. the frequency of the wave is 4 times the frequency of the resonator. In one period the wave has travelled the full domain. Due to the periodic boundary conditions, the wave re-enters the domain from the left with a reduced amplitude, both because of its natural decay due to viscosity and because of the interaction with the resonators. Therefore, the resonator oscillates with a decreasing amplitude (as highlighted in figure 3), since they are forced by waves whose amplitude is decreasing in time. In the inset of the figure we plot the wave amplitude (computed as the difference between the maximum and minimum value of the surface elevation) vs. time for the same cases: the simulation with  $\Omega = 1$  exhibits a stronger decrease of wave amplitude which is in line with an increase of dissipation, as discussed below.

We find very instructive to show the space-time plots of the surface elevation, displayed in figure 4. The presence of the resonator induces a local perturbation of the surface elevation; this is clearly visible in the top panel of figure 4, corresponding to the case with a fixed cylinder located at  $x/\lambda = 0.5$ . Additionally, when the solid body oscillates, the interaction with the propagating surface gravity wave leads to the generation of a wave travelling in the opposite direction with respect to the original one. This is highlighted in the middle panel of figure 4 by a brown line. For this simulation the period of the resonator is four times the wave period ( $\Omega = 0.25$ ) and after approximately four non-dimensional times there is an inversion of the direction of propagation of the wave, which is again recovered after four more wave periods. For the case  $\Omega = 1$ , bottom panel of figure 4, a similar dynamics takes place on a shorter time scale but the evolution of the free-surface is less regular.

In the following we will quantify the dissipated power during the wave propagation as a function of  $\Omega$  and the number of resonators per wavelength. Due to the non-stationary nature of the system, such measure must be described in a time-dependent fashion. When a surface gravity wave of small amplitude (*i.e.* small steepness  $\varepsilon = ak$ ) propagates freely, its total energy decays with an exponential rate equal

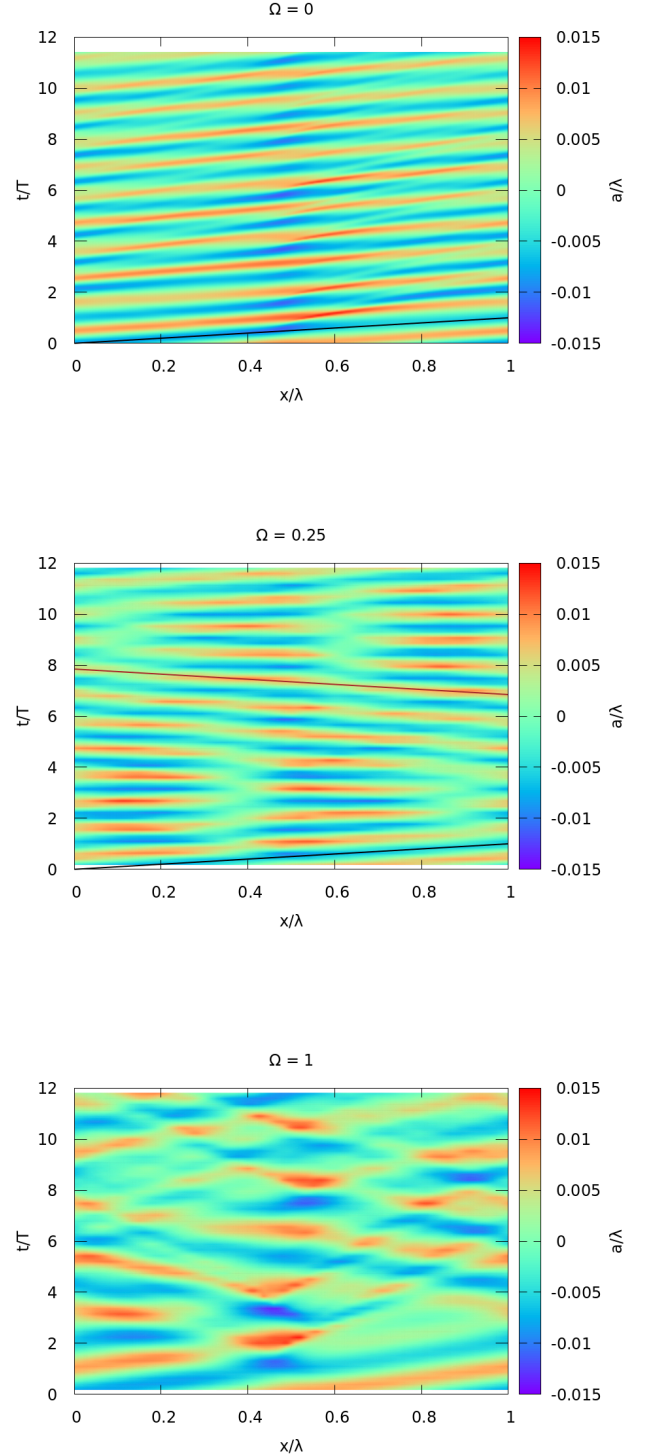


FIG. 4: Space-time evolution of the surface elevation: (top)  $\Omega = 0$ ; (middle)  $\Omega = 0.25$ ; (bottom)  $\Omega = 1$ . The two lines in the middle panel highlight forward (black line) and backward (brown line) propagating waves.

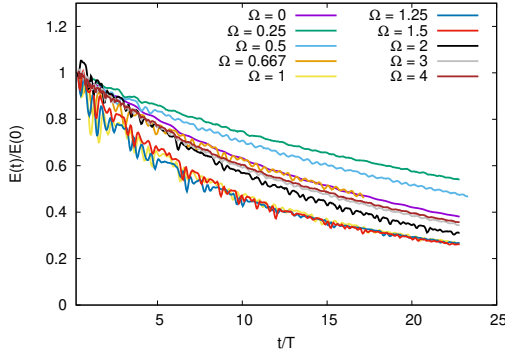


FIG. 5: Time history of the total energy vs the frequency ratio  $\Omega$  for the case of one single resonator.

to  $E(t) = E(0)e^{-2\gamma t}$ , as described by Landau and Lifshitz<sup>24</sup>. Here, the wave energy  $E(t)$  is the sum of the kinetic and potential contribution defined as:

$$E(t) = K(t) + U(t) = \frac{1}{2} \int_0^\lambda \int_{-h}^\eta \rho |\mathbf{u}|^2 dz dx + \int_0^\lambda \int_{-h}^\eta \rho g z dz dx - \bar{U} \quad (11)$$

where  $z = -h$  is the position of the flat bottom,  $z = \eta(x, t)$  is the displacement of the surface with respect to its equilibrium position and  $\bar{U} = \int_0^\lambda \int_{-h}^0 \rho g z dz dx = -\rho g \lambda h^2$  the potential energy of the still water level.  $E(0)$  is the initial energy budget of the wave and  $\gamma = 2\nu k^2$  is the decaying rate,  $\nu$  being the kinematic viscosity of the fluid. As mentioned, our aim is to evaluate the effect of the resonator on the propagation of the wave for different values of the frequency of the resonator  $\omega_r$ . If the oscillator were in vacuum or in a low density fluid, its frequency would simply be given by  $\omega_r = \sqrt{\kappa/m}$ ; however, because of the presence of a dense fluid, a proper evaluation of the latter needs to account also for the added mass given by the surrounding fluid which results in a frequency  $\omega_r = \sqrt{\kappa/(m + \rho_w \mathcal{V})}$ , with  $\mathcal{V}$  the volume of the resonator.

We start first by studying the interaction of a single resonator with the wave. Depending on the ratio  $\Omega$ , the energy transfer from the wave to the resonator can be more or less effective. The effectiveness of the energy transfer from waves to the resonators is more clearly visible in the total energy history of the wave displayed in figure 5. The plot shows that small and large values of  $\Omega$  are associated with smaller dissipation, whereas values of  $\Omega$  close to unity are more dissipative. In these cases, a large amount of energy is dissipated in few wave periods. To quantify the dissipation we have performed a fit of these curves with an exponential form  $E(t) \sim E(0) \exp[-Dt]$ . The coefficients of the fit are reported in figure 6, where we show the results for simulations with up to 4 resonators. The curves show a clear peak of dissipation around  $\Omega = 1$ . The plots include the results for arrays of fixed cylinders, labelled by  $\Omega = 0$ . Independently of the number of resonators, we observe a range of frequency ratios, between 0 and 1, for which the dissipation is smaller than for the case of fixed resonators. Such dip is particularly evident for the case with one resonator per wavelength and is reduced

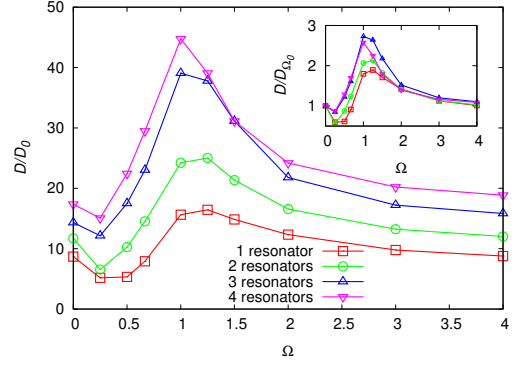


FIG. 6: Dissipation coefficient  $D$  normalised with the value for simple travelling wave  $D_0$  vs the frequency ratio  $\Omega$  for different number of oscillators. In the inset the same data are reported normalised with respect to the dissipation corresponding to the case of fixed cylinders  $D_{\Omega_0}$  (computed separately for each case).

when the number of cylinders is increased. The dissipation then increases and has a peak for  $\Omega \sim 1$ . For  $\Omega > 1$  it decreases and appears to approach an asymptote close to the value found for fixed cylinders. It is worth noticing that the curves in figure 6 resemble the curves reported for a system for wave energy conversion<sup>18</sup> in which the focus is on maximising the extracted power. This seems to indicate that the system of submerged resonators is a rather efficient system in dissipating wave power. As the number of resonators is increased, the dissipation also increases. However, this is not a trivial effect due to the total viscous drag of the cylinders on the fluid. Indeed, the ratio between the peak value of the dissipation (around resonance) and the fixed-cylinder value increases as the number of resonator increases between 1 and 3, and appears to decrease with 4 resonators. This suggests that non-trivial interaction effects are present. It is also interesting to observe that the width of the dissipation peak, and therefore the range of frequencies for which the dissipation is greater than the fixed-obstacle case, becomes wider. Therefore, decreasing the ratio between the wavelength of the wave and the wavelength of the periodic structures enlarges the range of frequencies for which an array of resonators produces a gain in dissipated power with respect to an array of fixed obstacles. An example of the flow field with four resonators and  $\Omega = 1$  is reported in figure 7. In this case the characteristic size of the perturbations induced by the resonators on the interface is of order of the size of the periodic structure. It is worth mentioning that, in the presence of a current, two main effects could be expected: *i)* because of the Doppler shift, the frequency of the wave can be shifted with respect to the one without a current; this would lead simply to a horizontal shift of figure 6; *ii)* The current may result in an extra force on the cylinder due to the exchange of the momentum between the current and the resonator. Clearly if the current is small compared to the velocities induced by the waves, the effect is negligible. However, in the case of strong current, the cylinder may enter into an overdamped regime and may not oscillate anymore. How-



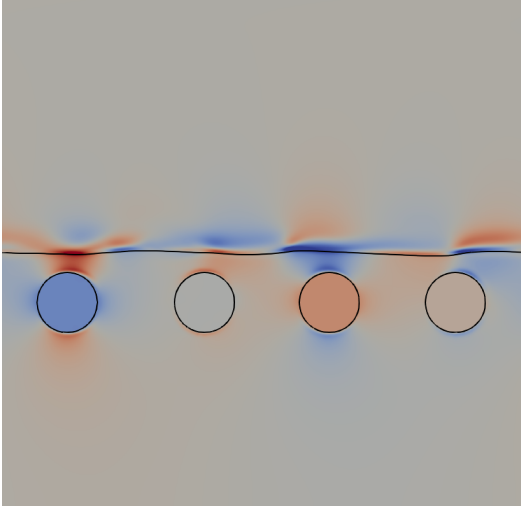


FIG. 7: Snapshots of the horizontal velocity component  $u$ , interface location and resonators position for the case with four resonators and  $\Omega = 1$  after one wave period. Colors as in figure 2. (Multimedia view)

ever, the present model can handle the presence of a current, since it will be included in the rhs of (6)

In figure 8 we report the time history of the centre of mass of the resonators for  $\Omega = 1$  and for different number of resonators. In the case of two oscillators (figure 8b), the curves have a Pearson correlation index of about -0.94 indicating that the oscillators are in phase opposition, as also clearly shown by the plot. For the case of three oscillators, instead, the correlation indexes of the curves are all about -0.5 because of a phase shift in the motion of the resonators (figure 8c). Finally, in the last case we find that the oscillators are correlated over a distance equal to  $\lambda/2$ , since the correlation coefficients for the first and third resonator, as well as that for the second and fourth, are about -0.97, while for the other pairs the coefficient is about 0.1.

#### IV. CONCLUSIONS

In this work, we have proposed to exploit the concept of mechanical metamaterials in the field of fluid mechanics, using of submerged resonators that interact with travelling waves, absorbing and dissipating mechanical energy. In order to properly describe the behaviour of the system, we have simulated the full Navier-Stokes equations for multiphase flows with fluid-structure interaction; this approach allows for a complete and detailed evaluation of hydrodynamic forces acting on the resonators and of the energy dissipation.

We have performed simulations in a periodic square domain of size equal to the wavelength of the wave, varying the elastic force acting on the resonators (*i.e.* their natural frequency) and the number of resonators per wavelength. We have computed the time history of the wave energy and found a dissipation coefficient by fitting the energy decay with an exponential form, similar to that of the viscous dissipation of a simple

travelling wave. By doing so, we have found that there is a peak of dissipation when the frequency of the wave and the frequency of the resonators approximately coincide. The dissipation observed at the peak is much larger than that caused by an array of fixed cylinders, so that the width of the peak represents the range for which the oscillatory dynamics (and, possibly, the fluid-mediated interaction among the structures) produces a gain in the dissipated power. Finally, the presence of a dissipation peak centred around a characteristic frequency suggests the presence of a band gap in the dispersion relations. The width of such band gap should increase with the number of resonators.

Future work will focus on coupling this system with a numerical wave maker to properly evaluate the dispersion relation and also to investigate the effect of resonator masses on the band gap. Additionally, the extension of the method to deformable solid bodies could open the field of applications also to flexible underwater structures. This work could open new applicative possibilities to realize low-cost, minimally invasive devices for ocean wave attenuation, contributing to reduced coastal erosion or protection of infrastructure such as offshore platforms or harbours.

#### DATA AVAILABILITY

The data that support the findings of this study are available from the corresponding author upon reasonable request.

#### ACKNOWLEDGMENTS

M. Onorato, F. De Lillo and F. De Vita have been funded by Progetto di Ricerca d'Ateneo CSTO160004, by the "Departments of Excellence 2018/2022" Grant awarded by the Italian Ministry of Education, University and Research (MIUR) (L.232/2016). The authors acknowledge the EU, H2020 FET Open BOHEME grant No. 863179 and CINECA for the computational resources under the grant IskraC SGWA.

<sup>1</sup>P. A. Deymier, "Introduction to phononic crystals and acoustic metamaterials," in *Acoustic metamaterials and phononic crystals* (Springer, 2013) pp. 1–12.

<sup>2</sup>M. I. Hussein, M. J. Leamy, and M. Ruzzene, "Dynamics of phononic materials and structures: Historical origins, recent progress, and future outlook," *Applied Mechanics Reviews* **66** (2014).

<sup>3</sup>J. Pendry, "Electromagnetic materials enter the negative age," *Physics World* **14**, 47 (2001).

<sup>4</sup>A. Davies and A. Heathershaw, "Surface-wave propagation over sinusoidally varying topography," *Journal of Fluid Mechanics* **144**, 419–443 (1984).

<sup>5</sup>T. Hara and C. C. Mei, "Bragg scattering of surface waves by periodic bars: theory and experiment," *Journal of Fluid Mechanics* **178**, 221–241 (1987).

<sup>6</sup>X. Hu, Y. Shen, X. Liu, R. Fu, and J. Zi, "Complete band gaps for liquid surface waves propagating over a periodically drilled bottom," *Physical Review E* **68**, 066308 (2003).

<sup>7</sup>X. Hu, C. Chan, K.-M. Ho, and J. Zi, "Negative effective gravity in water waves by periodic resonator arrays," *Physical review letters* **106**, 174501 (2011).

<sup>8</sup>P. Kar, T. Sahoo, and M. Meylan, "Bragg scattering of long waves by an array of floating flexible plates in the presence of multiple submerged trenches," *Physics of Fluids* **32**, 096603 (2020).

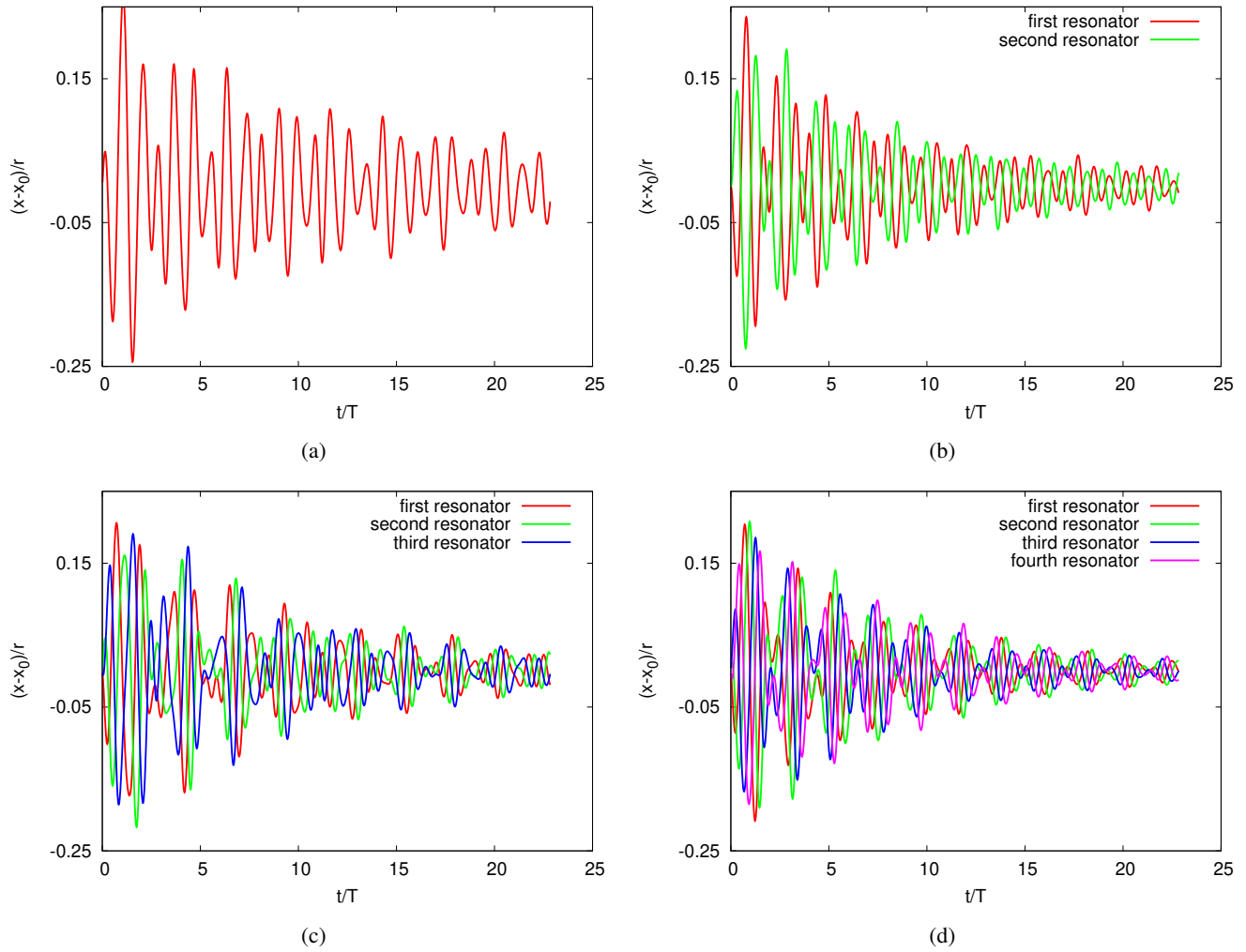


FIG. 8: Time history of the horizontal position of the centre of mass of the oscillators: (a) case with 1 resonator (b) case with two resonators; (c) case with three resonators; (d) case with four resonators. For all cases  $\Omega = 1$ .

- <sup>9</sup>A. Zareei and R. Alam, “Cloaking by a floating thin plate,” in *Proc. 31st Int. Workshop on Water Waves and Floating Bodies, Michigan, USA* (2016) pp. 197–200.
- <sup>10</sup>Z. Zhang, G. He, W. Wang, S. Liu, and Z. Wang, “Broadband cloaking of multiple truncated cylinders in water waves using the arrangement defects,” *Physics of Fluids* **32**, 067111 (2020).
- <sup>11</sup>C. C. Mei, *The applied dynamics of ocean surface waves*, Vol. 1 (World scientific, 1989).
- <sup>12</sup>H. Heikkinen, M. J. Lampinen, and J. Böling, “Analytical study of the interaction between waves and cylindrical wave energy converters oscillating in two modes,” *Renewable Energy* **50**, 150–160 (2013).
- <sup>13</sup>A. Abbasnia and C. G. Soares, “Fully nonlinear simulation of wave interaction with a cylindrical wave energy converter in a numerical wave tank,” *Ocean Engineering* **152**, 210 – 222 (2018).
- <sup>14</sup>S. Jin, R. J. Patton, and B. Guo, “Viscosity effect on a point absorber wave energy converter hydrodynamics validated by simulation and experiment,” *Renewable Energy* **129**, 500 – 512 (2018).
- <sup>15</sup>Q. Xu, Y. Li, Y. Xia, W. Chen, and F. Gao, “Performance assessments of the fully submerged sphere and cylinder point absorber wave energy converters,” *Modern Physics Letters B* **33**, 1950168 (2019).
- <sup>16</sup>Y. Li and Y.-H. Yu, “A synthesis of numerical methods for modeling wave energy converter-point absorbers,” *Renewable and Sustainable Energy Reviews* **16**, 4352–4364 (2012).
- <sup>17</sup>A. S. Zurkinden, F. Ferri, S. Beatty, J. P. Kofoed, and M. Kramer, “Non-linear numerical modeling and experimental testing of a point absorber wave energy converter,” *Ocean Engineering* **78**, 11–21 (2014).
- <sup>18</sup>M. Anbarsooz, M. Passandideh-Fard, and M. Moghiman, “Numerical simulation of a submerged cylindrical wave energy converter,” *Renewable Energy* **64**, 132–143 (2014).
- <sup>19</sup>J. Kim and P. Moin, “Application of a fractional-step method to incompressible Navier-Stokes equations,” *Journal of Computational Physics* **59**, 308–323 (1985).
- <sup>20</sup>C.-W. Shu, “High Order Weighted Essentially Nonoscillatory Schemes for Convection Dominated Problems,” *SIAM Review* **51**, 82–126 (2009).
- <sup>21</sup>E. A. Fadlun, R. Verzicco, P. Orlandi, and J. Mohd-Yusof, “Combined Immersed-Boundary Finite-Difference Methods for Three-Dimensional Complex Flow Simulations,” *Journal of Computational Physics* **161**, 35–60 (2000).
- <sup>22</sup>R. W. Hamming, “Stable Predictor-Corrector Methods for Ordinary Differential Equations,” (1959).
- <sup>23</sup>F. D. Vita, F. D. Lillo, R. Verzicco, and M. Onorato, “A fully eulerian solver for the simulations of multiphase flows with solid bodies: application on surface gravity waves,” arXiv:2006.05361.
- <sup>24</sup>L. D. Landau and E. M. Lifshitz, *Fluid Mechanics* (Pergamon Press, 1959).
- <sup>25</sup>K. Zhang, B. C. Douglas, and S. P. Leatherman, “Global warming and coastal erosion,” *Climatic change* **64**, 41 (2004).

- <sup>26</sup>E. C. Bird, *Coastal geomorphology: an introduction* (John Wiley & Sons, 2011).
- <sup>27</sup>L. Firth, R. Thompson, K. Bohn, M. Abbiati, L. Airoidi, T. Bouma, F. Bozzeda, V. Ceccherelli, M. Colangelo, A. Evans, *et al.*, “Between a rock and a hard place: environmental and engineering considerations when designing coastal defence structures,” *Coastal Engineering* **87**, 122–135 (2014).
- <sup>28</sup>F. Bulleri and L. Airoidi, “Artificial marine structures facilitate the spread of a non-indigenous green alga, *codium fragile* ssp. *tomentosoides*, in the north adriatic sea,” *Journal of Applied Ecology* **42**, 1063–1072 (2005).
- <sup>29</sup>F. Lalli, A. Bruschi, L. Liberti, V. Pesarino, and P. Bassanini, “Analysis of linear and nonlinear features of a flat plate breakwater with the boundary element method,” *Journal of fluids and structures* **32**, 146–158 (2012).
- <sup>30</sup>W. K. Lee and E. Y. Lo, “Surface-penetrating flexible membrane wave barriers of finite draft,” *Ocean engineering* **29**, 1781–1804 (2002).